Title
Examination of bioenergetic function in the inner mitochondrial membrane peptidase 2-like (Immp2l) mutant mice

Authors
Bharadwaj, Manish S
Zhou, Yu
Molina, Anthony J
et al.

Publication Date
2014

DOI
10.1016/j.redox.2014.08.006

Peer reviewed

Redox Biology 2 (2014) 1008–1015

Contents lists available at ScienceDirect

Redox Biology

journal homepage: www.elsevier.com/locate/redox

Research Paper

Examination of bioenergetic function in the inner mitochondrial membrane peptidase 2-like (*Immp2l*) mutant mice

Manish S. Bharadwaj [a], Yu Zhou [b], Anthony J. Molina [a], Tracy Criswell [b], Baisong Lu [b,*]

[a] Section on Gerontology and Geriatric Medicine, Wake Forest University Health Sciences, Department of Internal Medicine, Medical Center Boulevard, Winston-Salem, NC 27157, USA

[b] Wake Forest Institute for Regenerative Medicine, Wake Forest University Health Sciences, Medical Center Boulevard, Winston-Salem, NC 27157, USA

ARTICLE INFO

Article history:
Received 13 August 2014
Received in revised form
14 August 2014
Accepted 25 August 2014
Available online 28 August 2014

Keywords:
Immp2l
Cytochrome c1
GPD2
Complex III
Mitochondrial respiration

ABSTRACT

Inner mitochondrial membrane peptidase 2-like (IMMP2L) protein is a mitochondrial inner membrane peptidase that cleaves the signal peptide sequences of cytochrome c1 (CYC1) and mitochondrial glycerol phosphate dehydrogenase (GPD2). *Immp2l* mutant mice show infertility and early signs of aging. It is unclear whether mitochondrial respiratory deficiency underlies this phenotype. Here we show that the intermediate forms of GPD2 and CYC1 have normal expression levels and enzymatic function in *Immp2l* mutants. Mitochondrial respiration is not diminished in isolated mitochondria and cells from mutant mice. Our data suggest that respiratory deficiency is not the cause of the observed *Immp2l* mutant phenotypes.

Introduction

Cytochrome c1 (CYC1) and mitochondrial glycerol phosphate dehydrogenase (GPD2) are mitochondrial inner membrane proteins that need bipartite signal sequences to guide them to their final destination: the mitochondrial-targeting signal sequence and the mitochondrial inner membrane-targeting signal sequence. The mitochondrial targeting signal sequence guides the precursor proteins to the mitochondrial matrix, and is then cleaved by mitochondrial processing peptidase in the matrix. The mitochondrial inner membrane-targeting signal sequence guides the intermediate proteins to the inner membrane, and is finally cleaved by mitochondrial inner membrane peptidase. Yeast mitochondrial inner membrane peptidase has one noncatalytic subunit Som1p [1], and two catalytic subunits Imp1p and Imp2p, each with non-overlapping substrates. Imp1p cleaves the mitochondrial inner membrane-targeting signal sequences from cytochrome c oxidase subunit 2 (Cox2p), cytochrome b2 (Cyb2p), NADH-cytochrome b5 reductase (Mcr1p) and mitochondrial glycerol-3-phosphate dehydrogenase (Gut2p) [2–5], whereas Imp2p cleaves the signal sequence from cytochrome c1 [6].

Mammalian IMMP1L and IMMP2L are homologs of yeast Imp1p and Imp2p [7,8]. Mouse IMMP2L has two substrates, CYC1 and GPD2 [9]. However, in yeast, Gut2p (a homolog of GPD2) is a substrate for Imp1p [5]. Substrates for mammalian IMMP1L have not been described, although mammalian DIABLO/SMAC was suggested as an IMMP1L substrate [8]. Yeast Imp1p substrate Cyb2p lacks a mammalian ortholog. Yeast Imp1p substrates Cox2p and Mcr1p have mammalian orthologs, but appear to lack a typical cleavable signal peptide sequence [10].

Immp2l mutant mice show a series of abnormalities in different organs, which can be classified as either age- dependent or -independent. Age-independent phenotypes include infertility and reduced food intake, which are proposed to be caused by superoxide negation of nitric oxide [9,11]. Age-dependent phenotypes include spermatogenic damage in male mice [12], bladder dysfunction [13], and ataxia in old mutant mice but not in age-matched normal control mice [14]. These phenotypes are proposed to be caused by chronic oxidative stress resulting from increased mitochondrial superoxide generation. While the oxidative stress hypothesis is consistent with the observed phenotypes, it remains unclear whether the phenotypes are caused by functional deficiency of IMMP2L substrates.

CYC1 is one of the 11 subunits of complex III (ubiquinol-cytochrome-c reductase) [15], which is located on the

Abbreviations: IMMP2L, inner mitochondrial membrane peptidase 2-like; CS, citrate synthase; CYC1, cytochrome c1; ECAR, extracellular acidification rate; GAPDH, glyceraldehyde 3-phosphate dehydrogenase (GAPDH); GPD2, mitochondrial glycerol phosphate dehydrogenase; OCR, oxygen consumption rate; VDAC1, voltage-dependent anion channel 1; complex III, ubiquinol-cytochrome-c reductase; complex I:NADH, ubiquinone oxidoreductase; complex II, succinate-ubiquinone oxidoreductase

* Corresponding author.
E-mail address: blu@wakehealth.edu (B. Lu).

http://dx.doi.org/10.1016/j.redox.2014.08.006

mitochondrial inner membrane involved in mitochondrial electron transfer. Ubiquinol from complex I (NADH:ubiquinone oxidoreductase) and complex II are oxidized by mitochondrial complex III to reduce cytochrome c, where CYC1 is the subunit transferring the electron to cytochrome c [16]. In yeast, the intermediate form of Imp2p substrate Cyt1p (i-Cyt1p, with the inner membrane targeting signal sequence uncleaved) has normal localization in the mitochondria and is respiratory competent [6]. However, the N-terminal signal peptide sequences of yeast Cyt1p and its mouse homolog CYC1 show little homology, and the entire mature sequences are only 58% identical. In addition, yeast and mouse complex III have different numbers of subunits [17]. Furthermore, patients with *CYC1* missense point mutations showed reduced complex III activity and insulin-responsive hyperglycemia [18]. Thus, it remains unclear whether the enzymatic function of the intermediate form of CYC1 (i-CYC1) is affected in *Immp2l* mutant mice.

GPD2, another IMMP2L substrate, catalyzes the conversion of glycerol-3-phosphate to dihydroxyacetone phosphate, reducing the enzyme-bound FAD. Together with the cytosolic glycerol phosphate dehydrogenase (GPD1), they form the glycerol phosphate shuttle, which uses the interconversion of glycerol-3-phosphate and dihydroxyacetone phosphate to transfer reducing equivalents into mitochondria, resulting in the reoxidation of NADH formed during glycolysis. It also remains unclear whether the enzymatic activity of GPD2 is impaired in *Immp2l* mutant mice due to the presence of uncleaved signal sequences.

The present study was designed to address questions regarding the enzymatic activities of IMMP2L substrates in *Immp2l* mutant mice. We find that CYC1 and GPD2 are functional in *Immp2l* mutant mice and conclude that mitochondrial respiration deficiency is not the cause of the observed phenotypes.

Materials and methods

Animals

The development and characterization of the *Immp2l* mutant mice has been described previously [9]. Mice were housed in the pathogen-free animal facility of Wake Forest University Health Sciences. Experiments were conducted in accordance with the National Research Council publication Guide for Care and Use of Laboratory Animals, and approved by the Institutional Animal Care and Use Committee of Wake Forest University Health Sciences. Mice were kept in microisolator cages with 12-h light/dark cycles and were fed *ad libitum*. Genotypes of the mice were determined by coat color. Normal homozygous mice (+/+) were albino due to the FVB background. Heterozygotes (+/−) were slightly pigmented due to the expression of tyrosinase from one copy of the transgene. Homozygous mutant mice (−/−) were darkly pigmented due to the expression of tyrosinase from both copies of the transgene. Mice were fed a chow diet (Prolab, RMH3000).

Quantitative RT-PCR analysis of gene expression

Total RNA was extracted from hypothalamic tissues with Turbo DNase (Ambion) to eliminate DNA contamination, and reverse transcribed as described previously [19]. Primer sequences for mouse *Dock4*, *Lrrn3*, *Dnajb9*, *Immp2l* exons 3–6 and *Immp2l* exons 3–7 have been described previously [9]. *Pbip* gene was used as the internal control, and primer sequences were tcgtctttggactctttggaa (forward primer) and agcgctcaccatagatgctc (reverse primer). RNA from 4 control and 4 mutant mice were compared. Each sample was assayed three times.

Preparation of mitochondrial and cytosolic proteins from mouse tissues

Testicular and brown fat tissues were excised from 2 to 3-month-old mice. Mitochondrial and cytosolic proteins were prepared as described previously [20]. Protease inhibitors (0.5 mM PMSF and 1 × Complete Protease Inhibitor Cocktail from Roche) were included to prevent protein degradation.

SDS-PAGE and Western blot analyses

Tissue extracts were prepared from 2 to 3-month-old mice in RIPA buffer including protease inhibitors. Mitochondrial, cytosolic proteins, and tissue extracts were separated by SDS-PAGE, transferred to a nitrocellulose membrane, and incubated with anti β-actin (Sigma, 1:5000), anti-GAPDH (Abcam, 1:500), anti-CYC1 (ProteinTech Group, 1:1000), anti-GPD2 (Abnova, 1:500), anti-VDAC1 (Abcam, 1:2000). Horseradish peroxidase (HRP)-conjugated secondary antibodies were purchased from Pierce. Chemiluminescent reagents from Pierce were used to visualize the protein signals under the LAS-3000 system from Fujifilm. The Integrated Density function from ImageJ software was used to quantify the expression of individual proteins after normalization by β-actin or GAPDH (for cytosolic proteins or total tissue extracts) and VDAC1 (for mitochondrial proteins).

Oxygen consumption rate (OCR) of isolated mitochondria

Whole hind limb skeletal muscle from a control and an *Immp2l*$^{-/-}$ mouse (2–3 months) was used for mitochondria isolation, following the protocols described previously [21–23]. Mitochondrial protein concentrations were determined using the BCA protein assay kit (Thermo Scientific, Rockford, IL). Mitochondrial OCR was measured using a Seahorse XF24 Extracellular Flux Analyzer (Seahorse Biosciences, Billerica, MA). 10 mM succinate was used as the substrate with the addition of 2 μM rotenone; 5 μg mitochondrial protein was loaded in each well. Three to four replicates of each sample were analyzed for the mean and SD. Following an initial 7 min of equilibration, ADP (2 mM), oligomycin (2 μM), FCCP [carbonyl cyanide 4-(trifluoromethoxy) phenylhydrazone, 6 μM] and antimycin (2 μM) were added successively to achieve the final concentration as given in parentheses.

Mitochondrial citrate synthase (CS) activity

CS activity of isolated muscle mitochondria was assayed with the kit from Sigma (Cat no. CS0720), according to the manufacturer's instructions. Assays were performed at 25 °C in a 96-well plate with 4 μg mitochondrial protein per well. Formation of 5-thio-2-nitrobenzoic acid was monitored with a SpectraMax M5 Microplate Reader (Molecular Devices, Sunnyvale, CA) at 412 nm. Before and after the addition of oxaloacetate, absorbance was monitored for 3 min. The difference of the slopes was calculated to obtain the CS specific activity. CS activity was calculated based on the TNB extinction coefficient of 13.6 mM^{-1} cm^{-1} at 412 nm. The pathlength of 0.553 cm was adopted for the 200 μl reaction in the 96-well plate.

2.7. Mitochondrial complex III activity

Mitochondrial complex III activity was assayed as described previously [24]. To prepare decylubiquinol, 10 mg decylubiquinone (Sigma, D7911) dissolved in 400 μl of nitrogen-saturated hexane was mixed with 400 μl of 1.15 M sodium dithionite, and vortexed until colorless. The organic phase was collected, and the decylubiquinol was recovered by evaporating the hexane under nitrogen.

The decylubiquinol was dissolved in 1 ml ethanol (acidified with 10 mM HCl) and stored in aliquots at −80 °C. Oxidized cytochrome c was from Sigma (C3131). 300 μl reaction mixture (15 μg mitochondrial protein and 60 μM cytochrome c) was added to a cuvette. After the addition of 3 μl decylubiquinol (stock concentration 15 mM, final concentration about 150 μM), reduction of cytochrome c was monitored at 550 nm once every second for 1 min with a SpectraMax M5 Microplate Reader (the chamber temperature was set at 30 °C). The assay was repeated with the addition of 1 μg Antimycin A (Sigma, A8674). Antimycin A-sensitive activity was calculated for the complex III activity. The extinction coefficient of cytochrome c is 21 mM^{-1} cm^{-1}.

Mitochondrial GPD2 activity

Isolated mitochondria from mouse skeletal muscle were frozen and thawed. GPD2 activity was determined by methods described by Dawson et al. [25] with the addition of complexes I, II, and III inhibitors as described by Orr et al. [26]. The assay was run in a 96-well plate, and each well contained 40 μg total mitochondrial protein in a total volume of 200 μl. The reaction mixture contained 50 mM KH_2PO_4–NaOH buffer (pH 7.6), 25 mM-L-3-glycerophosphate, 50 μM DCPIP (2,6-dichlorophenolindophenol, Sigma), 4 μM rotenone, 2.5 μM antimycin A, and 1 mM malonate. The assay was started by the addition of mitochondrial proteins, and the decrease in absorption at 600 nm was recorded by a SpectraMax M5 Microplate Reader (Molecular Devices, Sunnyvale, CA) pre-warmed to 37 °C. The progress curve was linear during the first 3–5 min; data from the first 3 min were used to determine the reaction velocity. The reduction of absorption at 600 nm in the absence of mitochondrial protein was negligible. Extinction coefficient of DCPIP at 600 nm was taken to be 21 mM^{-1} cm^{-1}.

Skeletal muscle myoblasts isolation, myotube differentiation, and oxygen consumption analysis

Myoblasts were isolated from two pairs of young control and mutant mice (aged 6 months), and three pairs of age-matched old control and mutant mice (aged 22, 25 and 29 months), following the procedures described previously [27] but with modifications. The proliferation medium contained Dulbecco's Modified Eagle Medium (DMEM) supplemented with 20% fetal bovine serum, 10% horse serum, 1% chicken embryo extract, and 5 ng/ml bFGF, and the differentiation medium contained 10% horse serum without bFGF. Four to five days after isolation, the myoblasts were collected and filtered through a cell strainer to remove debris. The cells were further re-suspended in proliferation medium, seeded in V7 cell culture plates (Seahorse Biosciences, Billerica, MA) (coated with 1:60 diluted Matrigel) at a concentration of 10^4 cells/well. After 3–4 days of proliferation, the medium was changed to differentiation medium for another one to two days. The cells were then analyzed with a Seahorse XF24 Extracellular Flux Analyzer as described previously [28]. Five to 11 replicates of each sample were analyzed for the mean and SD. Cells were incubated in Seahorse XF assay media with 5.56 mM D-Glucose, 1 mM sodium pyruvate, and 2 mM glutamax-1 added then pH titrated to 7.4 using NaOH. Following an initial 36 min of equilibration, oligomycin (0.75 μM), FCCP (1.0 μM), and antimycin (1.0 μM) plus rotenone (1 μM) were added successively to achieve the final concentrations (shown in parentheses). OCR (oxygen consumption rate) and extracellular acidification rate (ECAR) were normalized to total protein obtained using a BCA kit after Seahorse analysis.

Statistical analysis

Two-tailed Student's *t*-tests were performed to compare means of two groups. Tukey's post-tests following analysis of variance (ANOVA) were performed for means of more than two groups. Paired *t*-tests were also performed to compare mitochondrial GPD2 activities. For measurements with more than one variant, two-way ANOVA was performed followed by Bonferroni post-tests. $P < 0.05$ was accepted as statistically significant.

Results

Immp2l gene but not adjacent genes are affected in Immp2l$^{-/-}$ mice

In *Immp2l* mutant mice, a transgenic insertion in intron 6 causes a 50 kb deletion in this 250 kb-intron [9] (Fig. 1A). The result is the disruption of normal expression of *Immp2l* mRNA after exon 6. *Immp2l* transcripts 5′ to exon 7 can be detected, but full-length *Immp2l* mRNA is undetectable. Three genes, *Dock4*, *Lrrn3*, and *Dnajb9*, are near this affected region, and *Lrrn3* is within intron 4 of *Immp2l*. Although mRNA of all the three genes was detected by non-quantitative RT-PCR [9], it is unclear whether their expression level could be affected. Here we used quantitative RT-PCR to further examine whether the expression levels of the adjacent genes are affected, which could not be answered by non-quantitative RT-PCR. Since *Lrrn3* is mainly expressed in the brain [29], brain expression of the three genes in *Immp2l* mutant mice was compared by quantitative RT-PCR (qRT-PCR). No significant differences were observed in the expression levels of the genes between control and mutant mice (Fig. 1). Consistent with

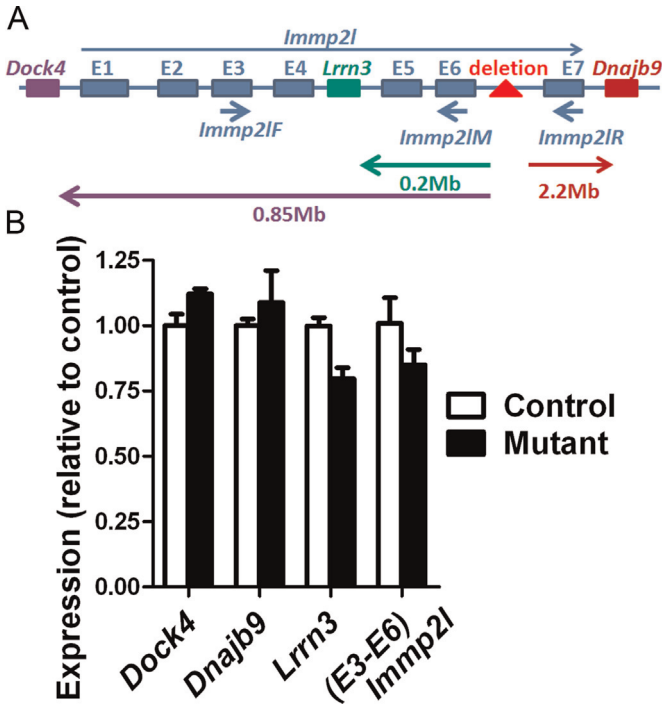

Fig. 1. Expression of *Immp2l* but not other nearby genes is affected in *Immp2l* mutant mice. (A) Genes in the affected region. E1–E7 are the seven exons of *Immp2l* gene. The red triangle in intron 6 indicates the location of the foreign DNA insertion and the 50-kb deletion. Short arrows indicate the location of the primers used for qRT-PCR. Long arrows indicate the distances between the deletion and the adjacent genes. The diagram was not drawn to scale. (B) qRT-PCR comparison of expression of genes in the same region as *Immp2l*. Four control and three mutant mice were analyzed. Means ± SEM are presented. No significant differences were found by ANOVA. (For interpretation of the references to color in this figure legend, the reader is referred to the web version of this article.)

our previous detection of truncated but not full-length *Immp2l* transcripts in RT-PCR analysis, *Immp2l* primers spanning exons 3 and 6 (Immp2lF and Immp2lM) detected similar expression between control and mutant mice in qRT-PCR (Fig. 1B). *Immp2l* primers spanning exons 3 and 7 (Immp2lF and Immp2lR) could only detect specific amplification from normal control mice (threshold cycle C_t=29 cycles), but not from mutant mice (C_t > 37 cycles).

IMMP2L substrate proteins have normal expression and compartmentalization in Immp2l$^{-/-}$ mice

Immp2l is expressed in all tissues, and its mutation affected CYC1 processing in all tissues examined in our previous study [9]. Mitochondrial and cytoplasmic proteins were prepared from mutant mice to determine whether the inability to cleave the signal sequence of CYC1 and GPD2 (the two known IMMP2L substrates) could affect the compartmentalization and expression of these two proteins. GPD2 has relatively high expression in brown adipose tissue [30]. We prepared mitochondrial and cytosolic proteins from brown adipose tissue of control and mutant mice; GPD2 was found in the mitochondrial but not the cytosolic fractions (Fig. 2A). CYC1 is widely expressed in all tissues. We examined CYC1 in the testis, an organ affected in *Immp2l*$^{-/-}$ mice [9,12]. Like GPD2, it was also detected in the mitochondrial but not the cytosolic fractions (Fig. 2A), demonstrating that the proteins are properly translocated to the mitochondria. This is consistent with observations in yeast, where the intermediate form of Cyt1p (i-Cyt1p) is correctly localized in the mitochondria of *IMP2* (the *Immp2l* homolog) mutant yeast [6]. Compared with voltage-dependent anion channel 1 (VDAC1), a mitochondrial outer membrane protein, IMMP2L substrates showed similar expression between control and mutant mice, in the tissues examined (testis and muscle for CYC1, brown adipose tissue for GPD2, Fig. 2A and B). These data showed that loss of IMMP2L activity does not affect the expression or the compartmentalization of CYC1 and GPD2.

A previous study reported no differences in qPCR analyses of mitochondrial DNA content between testicular cells of control and mutant mice [12], suggesting that the *Immp2l* mutation does not affect total mitochondrial mass of testicular cells. Western blot was performed to compare mitochondrial content in more tissues from control and mutant mice. We analyzed VDAC1 expression relative to glyceraldehyde 3-phosphate dehydrogenase (GAPDH), a cytosol protein, in muscle and liver tissue lysates from 5-month-old mice. The VDAC1/GAPDH density ratios in mutant mice were similar to those of control mice, indicating no mitochondrial mass deficiency in young mutants (Fig. 2C and D). Ratios also were similar between control and mutant mice at the age of 24 months.

Mitochondria of mutant mice have normal complex III activity

CYC1 is one of the three redox centers of mitochondrial complex III. Skeletal muscle is a common source of mitochondria for mitochondrial complex activity analysis. We wondered whether the intermediate form of CYC1 (i-CYC1) could compromise the ubiquinol:cytochrome c oxidoreductase activity of mitochondria from mutant mice. The size of CYC1 in muscle mitochondria from mutant mice (Fig. 2B) confirmed that it is an intermediate form (i-CYC1). We found no differences in CS and complex III activities of muscle mitochondria from control and mutant mice (Fig. 3A). The ratios of complex III/CS were also similar (Fig. 3B). Cells from *CYC1* mutant patients show reduced complex III activity [18]. Normal complex III activity of mitochondria from mutant mice suggests that i-CYC1 protein is enzymatically active.

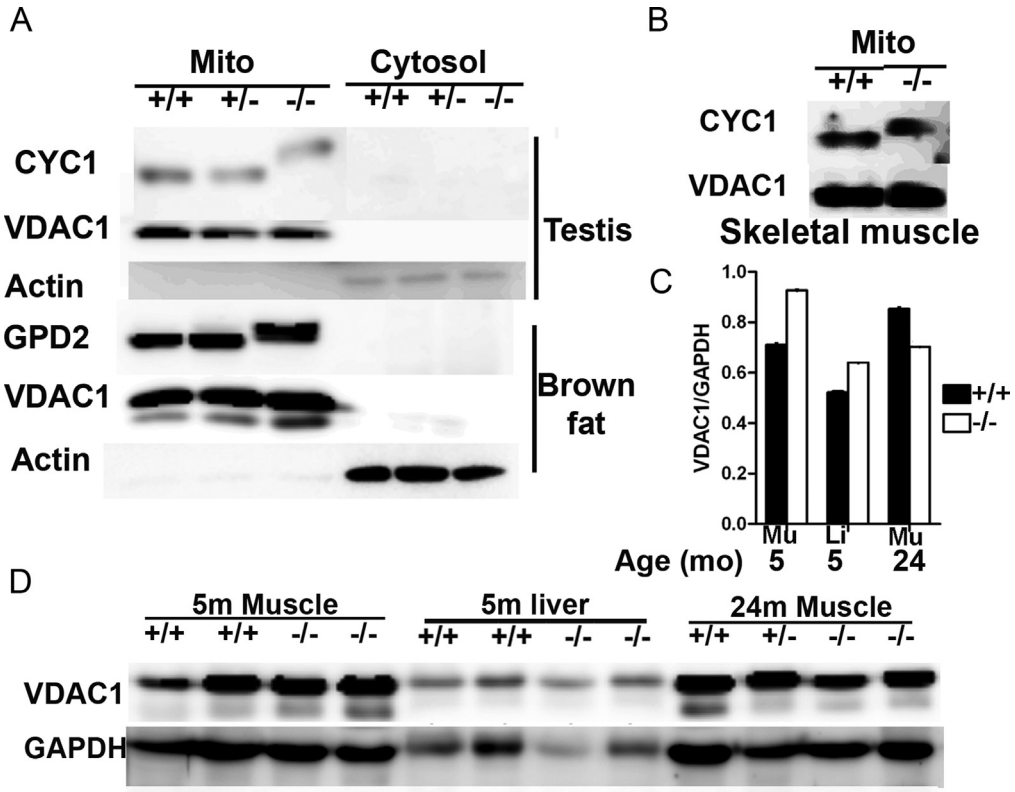

Fig. 2. Expression of IMMP2L substrates in *Immp2l* mutant mice. (A) CYC1 and GPD2 expression determined by Western blot analyses in 3–5-month-old mutant mice. VDAC1 and β-actin were used as mitochondrial and cytosolic markers, respectively. (B) CYC1 expression in muscle mitochondria from 3 to 5-month-old mutant mice. (C) Densitometry comparison of VDAC1 expression in muscle and liver of control and mutant mice. Data were derived from panel "D". Means ± SEM are presented. Mu: skeletal muscle; Li: Liver. (D) Western blot analyses of VDAC1 expression between control and mutant mice using whole tissue lysates. GAPDH was used as a loading control.

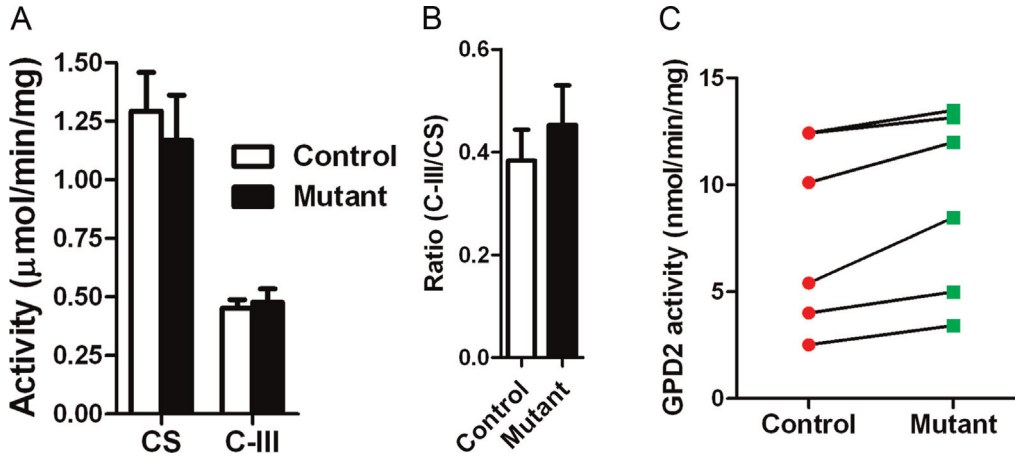

Fig. 3. Normal complex III and CS activities of mutant mice. (A) Complex III and CS activities of control and mutant mice. Means ± SEM of six mice (3–5 months) are presented. Complex III activity was expressed as the amount cytochrome c reduced in μmol/min/mg. CS activity was expressed as the amount of 5-thio-2-nitrobenzoic acid (TNB) formed in μmol/min/mg. Differences were not statistically significant between control and mutant mice by ANOVA. (B) Similar complex III/CS activity ratios between controls and mutants. No statistically significant differences were found by *t*-test ($p=0.49$). (C) GPD2 activity of mitochondria from control and mutant mice. Measurements were done with the same mitochondrial preparations used for complex III activity assay. Values linked by lines were from mitochondria preparations from littermates sacrificed on the same dates.

Mitochondria of mutant mice have normal GPD2 activity

No difference was observed in GPD2 activity in frozen/thawed muscle mitochondria between control and mutant mice (7.81 ± 1.79 nmol/min/mg, $N=6$ from control mice; 9.25 ± 1.76 nmol/min/mg, $N=6$ for mutant mice; $p=0.58$ by *t*-test). Mitochondrial samples were isolated on different days from one control and one mutant mouse (littermates) for experiments requiring fresh mitochondria. We noticed that GPD2 activity shows relatively large intra-group variations. This could be caused by the fact that mice of the same genotype were sacrificed at different dates for tissue collection. Supporting our reasoning, tissues from control and mutant mice sacrificed at the same days had similar values. When compared by paired *t*-test, mitochondria from mutant mice showed even higher GPD2 activity ($p=0.0109$, paired *t*-test). The data exclude GPD2 enzymatic deficiency in mutant mice.

Mitochondrial respiration of mutant mice is not diminished

Isolated mitochondria from skeletal muscle of 3–5-month-old control and mutant mice were analyzed for their oxidative phosphorylation. Mitochondria from control and mutant mice had similar oxygen consumption rates (OCRs) at all states: when only substrate is present (state 2); when respiration is stimulated by addition of ADP to stimulate ATP synthesis or uncoupling reagent FCCP, allowing the inward flow of protons across the inner membrane without ATP synthesis, and when respiration is inhibited by ATP synthase inhibitor oligomycin or complex III inhibitor antimycin A (Fig. 4). No defects of oxidative phosphorylation were noted in mitochondria isolated from mutant mice.

Respiration and glycolysis of myoblast-derived skeletal muscle myotubes from mutant mice are normal

Myoblasts were isolated from skeletal muscles of control and mutant mice and differentiated into myotubes. The OCR (reflecting mitochondrial respiration) and extracellular acidification rate (ECAR, reflecting glycolysis) were compared between myotubes differentiated from myoblasts of control and mutant mice. Differentiated myotubes from 6-month-old mutant mice had similar OCR and ECAR traces as myotubes from their age-matched controls (Fig. 5A and B). Cell numbers were confirmed as similar by

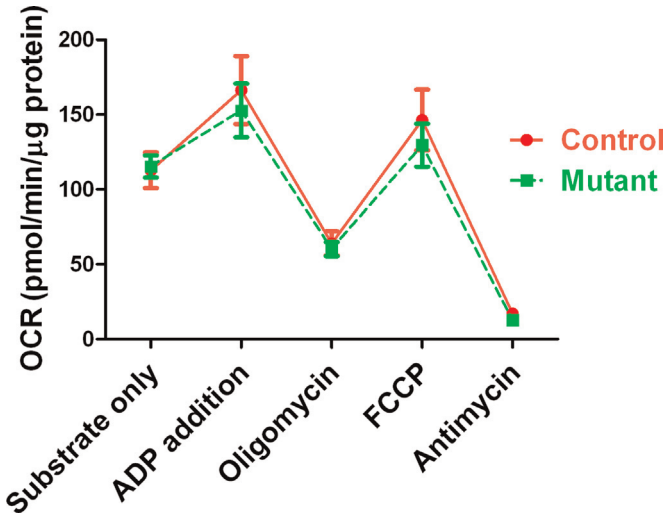

Fig. 4. Normal mitochondrial respiration of *Immp2l* mutant mice. Mean ± SEM of 5 pairs are presented. No significant difference was found by ANOVA.

determining protein concentrations after the Seahorse reading. The data suggest that cells from control and mutant mice have similar rates of mitochondrial respiration and glycolysis. Similar observations were made in differentiated myotubes from 22–29-month-old control and mutant mice (Fig. 5C and D).

Discussion

CYC1 and GPD2 are two known substrates for IMMP2L, a peptidase on the mitochondrial inner membrane that cleaves the space-sorting signal sequences from the precursors of its substrates. The signal peptide sequences of CYC1 and GPD2, also mitochondrial inner membrane proteins, remain unprocessed in *Immp2l* mutant mice [9]. *Immp2l* mutant mice show normal embryonic and postnatal development, but exhibit abnormalities in multiple systems, including infertility and a 30% reduced food intake [9,11]. In addition, some abnormalities, including bladder dysfunction [13], ataxia [14], and spermatogenic impairment [12], develop as mice age. Based on our observation of increased mitochondrial superoxide generation in the mutant mice, we

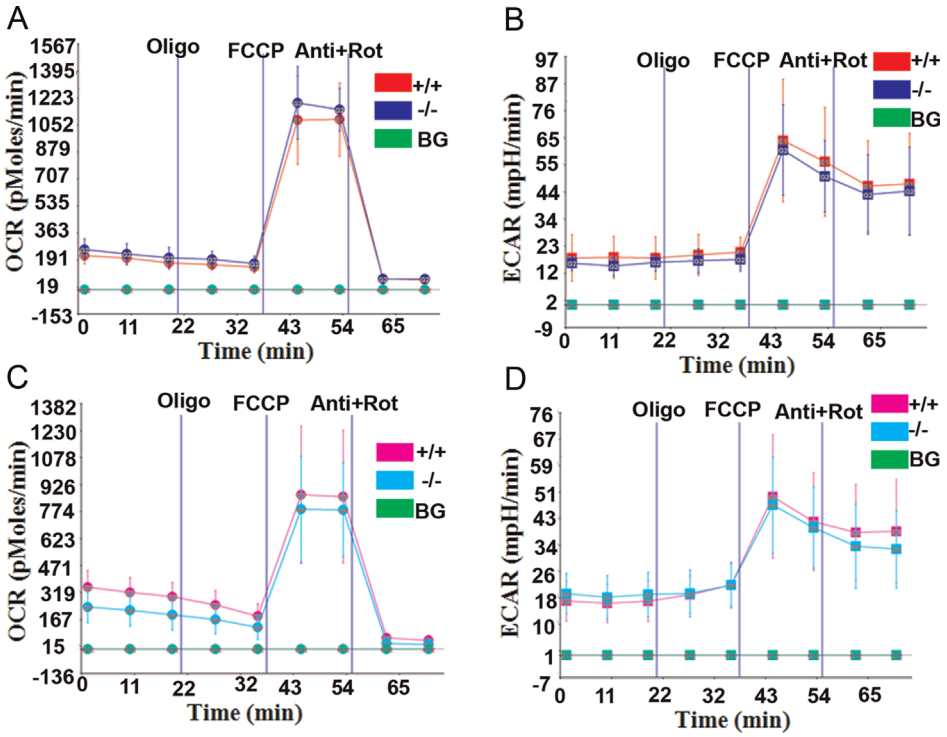

Fig. 5. Respiration and glycolysis of *in vitro* differentiated myotubes. (A and B) Representative OCR (A) and ECAR (B) traces of myotubes from two pairs of 6-month-old control and mutant littermates. Data shown are means ± SD of 5 replicates. (C and D) OCR (C) and ECAR (D) traces of myotubes from old mice. Traces were representative of three pairs of control and mutant littermates (aged 22, 25, and 29 months respectively). Presented were means ± SD of 6 replicates from mice of 22 months. Oligo: oligomycin; anti: antimycin; FCCP: carbonyl cyanide 4-(trifluoromethoxy) phenylhydrazone; Rot: rotenone; and BG: no cell background.

proposed that mitochondrial oxidative stress underlies these phenotypes. However, whether CYC1 and GPD2 activity deficiency also contributes to the observed mutant phenotype is not clear.

We confirmed that *Immp2l* expression is affected due to disruption of exon 7, the portion of *Immp2l* mRNA 3′ to the transgene insertion site. The adjacent genes, *Dock4*, *Lrrn3*, and *Dnajb9*, are not affected in the mutants. *Dock4* and *Dnajb9* knockout mice are unavailable; *Lrrn3* knockout mice have increased body fat and enhanced glucose tolerance (http://www.informatics.jax.org/marker/MGI:106036). These phenotypes are different from those of *Immp2l* mutant mice, suggesting that the *Lrrn3* gene does not contribute to the phenotype of *Immp2l* mutant mice.

CYC1 and GPD2 were both observed in the mitochondria but not the cytosol in mutant mice. In addition, CYC1 and GPD2 expression were not affected in the mutants. Thus, IMMP2L deficiency does not affect the expression of its substrates. Furthermore, mitochondria from mutant mice had normal complex III activity (CYC1 is a subunit of complex III) and higher than normal GPD2 activity. The intermediate forms of CYC1 and GPD2 are enzymatically functional, consistent with the observation that yeast i-cyt1p (a CYC1 homolog) is respiratory competent [6]. Furthermore, myofibers from mutant mice showed both normal oxygen consumption (an indication of mitochondrial respiration) and normal extracellular acidification rates (an indication of glycolysis). Considering our previous findings that mutant mice have normal complex I and complex II activities and cellular ATP levels [9], we conclude that the phenotype of *Immp2l* mutant mice is unlikely to be caused by mitochondrial respiratory deficiency. Most analyses were done with tissues from young mice. We think that this is appropriate since the primary cause must also be observed when young. We agree that examining old tissues may provide more information about the combined effects of the primary defects and age. However, using 2-year-old mice for these experiments is impractical considering the cost and time needed to generate the mice.

We used myofibers and skeletal muscle-derived mitochondria for respirometry analyses because these are common sources of materials for such analyses. Similar analyses using other tissues, especially those most affected in the mutants (e.g. the testis and the brain), could reinforce our argument. CYC1 from muscle lysates of mutant mice has larger than normal size, demonstrating that IMMP2L activity is lost in muscle tissues. We cannot examine the size of GPD2 in muscle lysates because of its relatively low expression in skeletal muscle. However, it is unlikely that GPD2 processing in muscle does not depend on IMMP2L activity. Since the intermediate forms of CYC1 and GPD2 are functional in skeletal muscle, it is logical that they are functional in other tissues.

This work suggests that respiratory deficiency is unlikely the cause of phenotypes observed in *Immp2l* mutant mice. Our previous works linked the abnormalities found in mutant mice to oxidative stress, either through superoxide negation of nitric oxide [9,11], or through detrimental effects of increased levels of reactive oxygen species [12–14]. Supporting our argument, we observed increased superoxide generation in mitochondria from mutant mice when using endogenous substrates [9]. In addition, multiple oxidative indices (carbonyl, 4-Hydroxynonenal) demonstrated oxidative stress in tissues from mutant mice [12,14]. Finally, testes from mutant mice have significantly increased catalase expression [12], consistent with increased superoxide generation and thus hydrogen peroxide levels.

Interestingly, complex III (of which CYC1 is a subunit) and GPD2 can generate superoxide as a byproduct [26,31–35]. Mutations in three of the 11 complex III subunits have been described in patients, but the pathological mechanism is unclear (MITOMAP: A Human Mitochondrial Genome Database. http://www.mitomap.org, 2013). GPD2 haploinsufficiency was described in a patient

with nonsyndromic mental retardation, but whether GPD2 was the cause is unclear [36]. However, conditional knockout of a gene coding for the Rieske iron–sulfur protein (a complex III subunit) in mice causes oxidative stress in the brain [37], confirming that perturbance of complex III can cause oxidative stress. We propose that retention of the signal sequences on CYC1 and/or GPD2 does not affect their ability for electron transfer, but increases the leakage of electrons to oxygen during electron transfer. It remains unknown how electron leakage is increased and whether CYC1 or GPD2 is the greater contributor to increased superoxide generation. We also cannot exclude the contribution of possible unidentified IMMP2L substrates.

In conclusion, the present work demonstrates that *Immp2l* mutant mice have no mitochondrial respiratory deficit, suggesting that respiratory deficiency is unlikely to be the cause of the observed *Immp2l* mutant phenotypes.

Acknowledgments

The authors thank Dr. Martin Brand (The Buck Institute for Research on Aging) for constructive discussions and Ms. Karen Klein (Translational Science Institute, Wake Forest University Health Sciences) for editing the manuscript. This work was partially supported by the National Institutes of Health (R01HD058058 to B. L.).

References

[1] K. Esser, E. Pratje, G. Michaelis, SOM 1, a small new gene required for mitochondrial inner membrane peptidase function in *Saccharomyces cerevisiae*, Molecular and General Genetics 252 (1996) 437–445 8879245.

[2] E. Pratje, B. Guiard, One nuclear gene controls the removal of transient presequences from two yeast proteins: one encoded by the nuclear the other by the mitochondrial genome, EMBO Journal 5 (1986) 1313–1317 3015596.

[3] K. Hahne, V. Haucke, L. Ramage, G. Schatz, Incomplete arrest in the outer membrane sorts NADH-cytochrome b5 reductase to two different submitochondrial compartments, Cell 79 (1994) 829–839. http://dx.doi.org/10.1016/0092-8674(94)90072-8 8001120.

[4] K. Esser, P.S. Jan, E. Pratje, G. Michaelis, The mitochondrial IMP peptidase of yeast: functional analysis of domains and identification of Gut2 as a new natural substrate, Molecular Genetics and Genomics 271 (2004) 616–626. http://dx.doi.org/10.1007/s00438-004-1011-y 15118906.

[5] W. Luo, H. Fang, N. Green, Substrate specificity of inner membrane peptidase in yeast mitochondria, Molecular Genetics and Genomics 275 (2006) 431–436. http://dx.doi.org/10.1007/s00438-006-0099-7 16450175.

[6] J. Nunnari, T.D. Fox, P. Walter, A mitochondrial protease with two catalytic subunits of nonoverlapping specificities, Science (New York, N.Y.) 262 (1993) 1997–2004. http://dx.doi.org/10.1126/science.8266095 8266095.

[7] E. Petek, C. Windpassinger, J.B. Vincent, J. Cheung, A.P. Boright, S.W. Scherer, P. M. Kroisel, K. Wagner, Disruption of a novel gene (IMMP2L) by a breakpoint in 7q31 associated with Tourette syndrome, American Journal of Human Genetics 68 (2001) 848–858. http://dx.doi.org/10.1086/319523 11254443.

[8] L. Burri, Y. Strahm, C.J. Hawkins, I.E. Gentle, M.A. Puryer, A. Verhagen, B. Callus, D. Vaux, T. Lithgow, Mature DIABLO/Smac is produced by the IMP protease complex on the mitochondrial inner membrane, Molecular Biology of the Cell 16 (2005) 2926–2933. http://dx.doi.org/10.1091/mbc.E04-12-1086 15814844.

[9] B. Lu, C. Poirier, T. Gaspar, C. Gratzke, W. Harrison, D. Busija, M.M. Matzuk, K. E. Andersson, P.A. Overbeek, C.E. Bishop, A mutation in the inner mitochondrial membrane peptidase 2-like gene (Immp2l) affects mitochondrial function and impairs fertility in mice, Biology of Reproduction 78 (2008) 601–610. http://dx.doi.org/10.1095/biolreprod.107.065987 18094351.

[10] N. Borgese, D. Aggujaro, P. Carrera, G. Pietrini, M. Bassetti, A role for N-myristoylation in protein targeting: NADH-cytochrome b5 reductase requires myristic acid for association with outer mitochondrial but not ER membranes, Journal of Cell Biology 135 (1996) 1501–1513. http://dx.doi.org/10.1083/jcb.135.6.1501 8978818.

[11] C. Han, Q. Zhao, B. Lu, The role of nitric oxide signaling in food intake; insights from the inner mitochondrial membrane peptidase 2 mutant mice, Redox Biology 1 (2013) 498–507. http://dx.doi.org/10.1016/j.redox.2013.10.003 24251118.

[12] S.K. George, Y. Jiao, C.E. Bishop, B. Lu, Oxidative stress is involved in age-dependent spermatogenic damage of Immp2l mutant mice, Free Radical Biology and Medicine 52 (2012) 2223–2233. http://dx.doi.org/10.1016/j.freeradbiomed.2012.04.003 22569411.

[13] R. Soler, C. Füllhase, B. Lu, C.E. Bishop, K.E. Andersson, Bladder dysfunction in a new mutant mouse model with increased superoxide—lack of nitric oxide? Journal of Urology 183 (2010) 780–785. http://dx.doi.org/10.1016/j.juro.2009.09.074 20022053.

[14] S.K. George, Y. Jiao, C.E. Bishop, B. Lu, Mitochondrial peptidase IMMP2L mutation causes early onset of age-associated disorders and impairs adult stem cell self-renewal, Aging Cell 10 (2011) 584–594. http://dx.doi.org/10.1111/j.1474-9726.2011.00686.x 21332923.

[15] D. González-Halphen, M.A. Lindorfer, R.A. Capaldi, Subunit arrangement in beef heart complex III, Biochemistry 27 (1988) 7021–7031. http://dx.doi.org/10.1021/bi00418a053 2848575.

[16] C. Hunte, H. Palsdottir, B.L. Trumpower, Protonmotive pathways and mechanisms in the cytochrome bc1 complex, FEBS Letters 545 (2003) 39–46. http://dx.doi.org/10.1016/S0014-5793(03)00391-0 12788490.

[17] U. Brandt, L. Yu, C.A. Yu, B.L. Trumpower, The mitochondrial targeting presequence of the Rieske iron–sulfur protein is processed in a single step after insertion into the cytochrome bc1 complex in mammals and retained as a subunit in the complex, Journal of Biological Chemistry 268 (1993) 8387–8390 8386158.

[18] P. Gaignard, M. Menezes, M. Schiff, A. Bayot, M. Rak, H. Ogier de Baulny, C. H. Su, M. Gilleron, A. Lombes, H. Abida, A. Tzagoloff, L. Riley, S.T. Cooper, K. Mina, P. Sivadorai, M.R. Davis, R.J. Allcock, N. Kresoje, N.G. Laing, D. R. Thorburn, A. Slama, J. Christodoulou, P. Rustin, Mutations in CYC1, encoding cytochrome c1 subunit of respiratory chain complex III, cause insulin-responsive hyperglycemia, American Journal of Human Genetics 93 (2013) 384–389. http://dx.doi.org/10.1016/j.ajhg.2013.06.015 23910460.

[19] Y. Jiao, C.E. Bishop, B. Lu, Mex3c regulates insulin-like growth factor 1 (IGF1) expression and promotes postnatal growth, Molecular Biology of the Cell 23 (2012) 1404–1413. http://dx.doi.org/10.1091/mbc.E11-11-0960 22357625.

[20] J. Yang, X. Liu, K. Bhalla, C.N. Kim, A.M. Ibrado, J. Cai, T.I. Peng, D.P. Jones, X. Wang, Prevention of apoptosis by Bcl-2: release of cytochrome c from mitochondria blocked, Science (New York, N.Y.) 275 (1997) 1129–1132. http://dx.doi.org/10.1126/science.275.5303.1129 9027314.

[21] S.K. Bhattacharya, J.H. Thakar, P.L. Johnson, D.R. Shanklin, Isolation of skeletal muscle mitochondria from hamsters using an ionic medium containing ethylenediaminetetraacetic acid and nagarse, Analytical Biochemistry 192 (1991) 344–349. http://dx.doi.org/10.1016/0003-2697(91)90546-6 1903610.

[22] S. Cadenas, K.S. Echtay, J.A. Harper, M.B. Jekabsons, J.A. Buckingham, E. Grau, A. Abuin, H. Chapman, J.C. Clapham, M.D. Brand, The basal proton conductance of skeletal muscle mitochondria from transgenic mice overexpressing or lacking uncoupling protein-3, Journal of Biological Chemistry 277 (2002) 2773–2778. http://dx.doi.org/10.1074/jbc.M109736200 11707458.

[23] J.B. Chappell, S.V. Perry, The respiratory and adenosinetriphosphatase activities of skeletal-muscle mitochondria, Biochemical Journal 55 (1953) 586–595 13115340.

[24] S. Krähenbühl, C. Talos, U. Wiesmann, C.L. Hoppel, Development and evaluation of a spectrophotometric assay for complex III in isolated mitochondria, tissues and fibroblasts from rats and humans, Clinica Chimica Acta: International Journal of Clinical Chemistry 230 (1994) 177–187. http://dx.doi.org/10.1016/0009-8981(94)90270-4 7834868.

[25] A.P. Dawson, C.J. Thorne, Preparation and some properties of L-3-glycerophosphate dehydrogenase from pig brain mitochondria, Biochemical Journal 111 (1969) 27–34 5775687.

[26] A.L. Orr, C.L. Quinlan, I.V. Perevoshchikova, M.D. Brand, A refined analysis of superoxide production by mitochondrial sn-glycerol 3-phosphate dehydrogenase, Journal of Biological Chemistry 287 (2012) 42921–42935. http://dx.doi.org/10.1074/jbc.M112.397828 23124204.

[27] M.E. Danoviz, Z. Yablonka-Reuveni, Skeletal muscle satellite cells: background and methods for isolation and analysis in a primary culture system, Methods in Molecular Biology (Clifton, N.J.) 798 (2012) 21–52. http://dx.doi.org/10.1007/978-1-61779-343-1_2 22130829.

[28] M. Wu, A. Neilson, A.L. Swift, R. Moran, J. Tamagnine, D. Parslow, S. Armistead, K. Lemire, J. Orrell, J. Teich, S. Chomicz, D.A. Ferrick, Multiparameter metabolic analysis reveals a close link between attenuated mitochondrial bioenergetic function and enhanced glycolysis dependency in human tumor cells, American Journal of Physiology. Cell Physiology 292 (2007) C125–C136. http://dx.doi.org/10.1152/ajpcell.00247.2006 16971499.

[29] H. Taniguchi, M. Tohyama, T. Takagi, Cloning and expression of a novel gene for a protein with leucine-rich repeats in the developing mouse nervous system, Brain Research Molecular Brain Research 36 (1996) 45–52. http://dx.doi.org/10.1016/0169-328X(95)00243-L 9011764.

[30] R.A. Koza, U.C. Kozak, L.J. Brown, E.H. Leiter, M.J. MacDonald, L.P. Kozak, Sequence and tissue-dependent RNA expression of mouse FAD-linked glycerol-3-phosphate dehydrogenase, Archives of Biochemistry and Biophysics 336 (1996) 97–104. http://dx.doi.org/10.1006/abbi.1996.0536 8951039.

[31] A. Herrero, G. Barja, Sites and mechanisms responsible for the low rate of free radical production of heart mitochondria in the long-lived pigeon, Mechanisms of Ageing and Development 98 (1997) 95–111. http://dx.doi.org/10.1016/S0047-6374(97)00076-6 9379714.

[32] J.F. Turrens, A. Alexandre, A.L. Lehninger, Ubisemiquinone is the electron donor for superoxide formation by complex III of heart mitochondria, Archives of Biochemistry and Biophysics 237 (1985) 408–414. http://dx.doi.org/10.1016/0003-9861(85)90293-0.

[33] C.J. Bolter, W. Chefurka, Extramitochondrial release of hydrogen peroxide from insect and mouse liver mitochondria using the respiratory inhibitors phosphine, myxothiazol, and antimycin and spectral analysis of inhibited

cytochromes, Archives of Biochemistry and Biophysics 278 (1990) 65–72. http://dx.doi.org/10.1016/0003-9861(90)90232-N 2321971.

[34] Z. Drahota, S.K. Chowdhury, D. Floryk, T. Mrácek, J. Wilhelm, H. Rauchová, G. Lenaz, J. Houstek, Glycerophosphate-dependent hydrogen peroxide production by brown adipose tissue mitochondria and its activation by ferricyanide, Journal of Bioenergetics and Biomembranes 34 (2002) 105–113. http://dx.doi.org/10.1023/A:1015123908918 12018887.

[35] Q. Chen, E.J. Vazquez, S. Moghaddas, C.L. Hoppel, E.J. Lesnefsky, Production of reactive oxygen species by mitochondria: central role of complex III, Journal of Biological Chemistry 278 (2003) 36027–36031. http://dx.doi.org/10.1074/jbc.M304854200 12840017.

[36] H. Daoud, N. Gruchy, J.M. Constans, E. Moussaoui, S. Saumureau, N. Bayou, M. Amy, S. Védrine, P.Y. Vu, A. Rötig, F. Laumonnier, P. Vourc'h, C.R. Andres, N. Leporrier, S. Briault, Haploinsufficiency of the GPD2 gene in a patient with nonsyndromic mental retardation, Human Genetics 124 (2009) 649–658. http://dx.doi.org/10.1007/s00439-008-0588-3 19011903.

[37] F. Diaz, S. Garcia, K.R. Padgett, C.T. Moraes, A defect in the mitochondrial complex III, But not complex IV, triggers early ROS-dependent damage in defined brain regions, Human Molecular Genetics 21 (2012) 5066–5077. http://dx.doi.org/10.1093/hmg/dds350 22914734.